



Photonic crystals for the visible range fabricated by autocloning technique and their application

T. SATO^{1*}, K. MIURA¹, N. ISHINO¹, Y. OHTERA¹, T. TAMAMURA²
AND S. KAWAKAMI¹

¹New Industry Creation Hatchery Center, Tohoku University, Aoba, Aramaki, Aoba-ku, Sendai, 980-8577 Japan;

²NTT Basic Research Laboratories, 3-1 Morinosato Wakamiya, Atsugi-shi Kanagawa Pref. 243-0198, Japan
(*author for correspondence: E-mail: sato@niche.tohoku.ac.jp)

Abstract. We fabricate photonic crystals for the visible range by the ‘autocloning’ technique, in which multilayers are stacked by an appropriate combination of sputter deposition and sputter etching. TiO₂/SiO₂ and Ta₂O₅/SiO₂ are chosen as materials since they are transparent in the range and give a high contrast of refractive indices. The fabrication technique has flexibility regarding materials and size and is very reliable and reproducible even if the pitch is less than 0.2 μm. We also study the application of photonic crystals to birefringent elements such as waveplates and polarization selective gratings and experimentally verify that they are useful for optical pick-up systems.

Key words: autocloning, birefringence, photonic crystal, polarization selective grating

1. Introduction

Photonic crystals are multi-dimensional periodic structures consisting of materials with different optical constants (Yablonovitch 1993) and characterized by useful optical properties such as band gap, strong anisotropy and high dispersion. The band gap has been studied for a long time for creating zero-threshold lasers and right-bending waveguides. On the other hand, the anisotropy and the dispersion, which are properties based on pass bands, have recently attracted much attention since they can also produce various useful applications, and thus band engineering, design of pass-band structure, becomes important for the applications.

We have proposed and studied a simple, useful fabrication technique of multi-dimensional [two-dimensional (2D) and 3D] photonic crystals, called autocloning (Kawakami 1997). The photonic crystals are composed of multilayers with surface periodic corrugation formed by a combination of sputter deposition and sputter etching. We have previously demonstrated practical devices such as polarizers by a 2D photonic crystal (Ohtera *et al.* 1999) and superprisms by a 3D photonic crystal (Kosaka *et al.* 1998) for the near infrared region by using a-Si and SiO₂.

In this paper, to expand the wavelength range from IR to visible range, we demonstrate autocloned photonic crystals in a new material system because

a-Si is absorptive in the range. We also experimentally verified that large birefringence is obtained by the band engineering and is applicable to components for optical pick-ups such as waveplates and polarization splitters.

2. Fabrication of photonic crystals

Fig. 1 shows a 2D autocloned photonic crystal using transparent materials in the visible range. The fabrication processes are as follows: after forming periodic grooves on a substrate by electron beam lithography and dry etching, multilayers composed of $\text{TiO}_2/\text{SiO}_2$ or $\text{Ta}_2\text{O}_5/\text{SiO}_2$ are stacked by a combination of sputter deposition and sputter etching using conventional bias-sputtering apparatus which has two targets and a substrate electrode, as shown in Fig. 2. When proper conditions are chosen so as to balance the effect of sputter deposition which narrows grooves and the effects of sputter

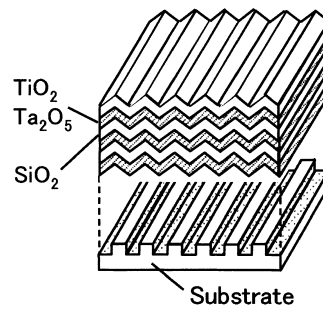


Fig. 1. Schematic illustration of 2D photonic crystal fabricated by autocloning.

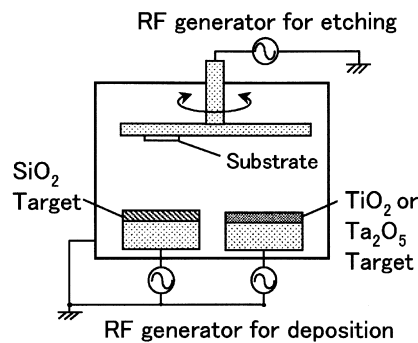


Fig. 2. Fabrication apparatus for the autocloning. Sputter deposition of two materials and sputter etching are carried out when rf power is fed to the targets and the substrate electrode, respectively.

etching which widens grooves, the stationary corrugation pattern is evolved from the initial pattern and is replicated automatically (Kawakami *et al.* 1999).

In this work, TiO_2 and Ta_2O_5 are chosen as high refractive index materials since they are known to be stable and easily obtained by sputter deposition. Fig. 3(a) and (b) show the refractive indices and absorption coefficient of the TiO_2 and Ta_2O_5 films. Here, TiO_2 and Ta_2O_5 films are deposited by sputtering a TiO_2 target in ambient Ar gas (2 mTorr) and by sputtering a Ta_2O_5 target in a mixture of Ar and O_2 gas ($\text{Ar}:\text{O}_2 = 9:1$, 1 mTorr), respectively. As the figure shows, TiO_2 is suitable for a larger refractive index while Ta_2O_5 is for lower loss and lower dispersion. Especially, use of Ta_2O_5 allows application at wavelengths as short as 400 nm.

Fig. 4(a) and (b) show the cross-sectional SEM photographs of the fabricated $\text{TiO}_2/\text{SiO}_2$ and $\text{Ta}_2\text{O}_5/\text{SiO}_2$ photonic crystals, respectively. The in-plane period L_x is 0.24 and 0.18 μm , and the lamination period L_z is 0.19 and 0.167 μm , respectively. These photos show that stationary corrugation patterns with a slope of more than 40° are successfully obtained, indicating that the method has high flexibility regarding size and materials.

Here, the initial rectangular grooves on the substrate are changed to the stationary triangular pattern since an SiO_2 film is formed by the autocloning process before stacking a multilayer. This results in reduction of scattering loss and low-loss light propagation in the normal direction (Kawashima *et al.* 2000), as shown in the measured transmission spectrum of the $\text{Ta}_2\text{O}_5/\text{SiO}_2$ crystal (Fig. 5(a)).

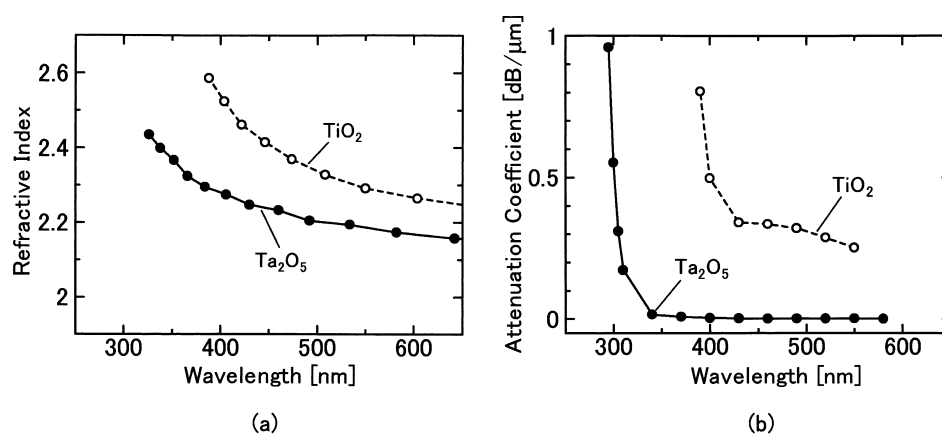


Fig. 3. (a) Refractive indices and (b) attenuation constants of TiO_2 and Ta_2O_5 films as high refractive index materials.

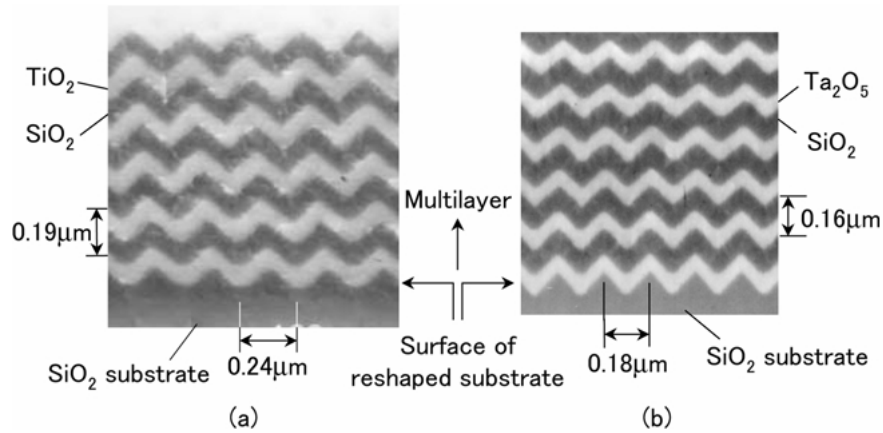


Fig. 4. Cross-sectional SEM photographs of (a) $\text{TiO}_2/\text{SiO}_2$ and (b) $\text{Ta}_2\text{O}_5/\text{SiO}_2$ photonic crystals. The initial rectangular grooves formed on a substrate are reshaped to the triangular grooves by deposition and etching of SiO_2 .

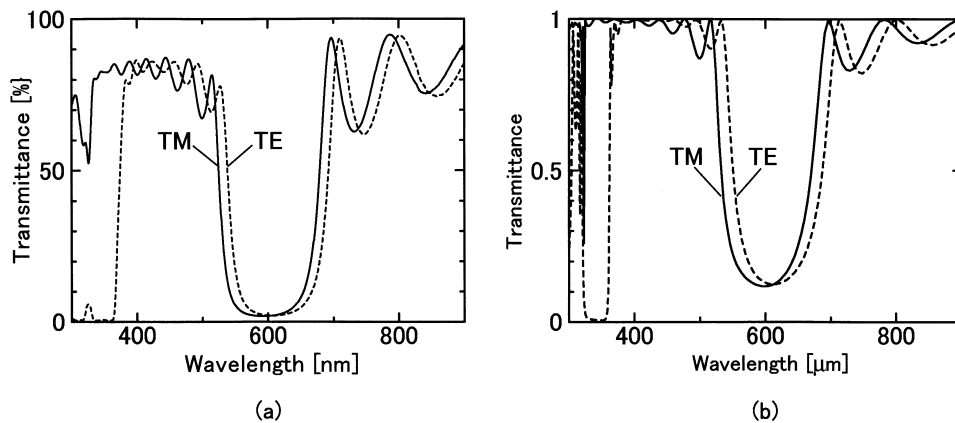


Fig. 5. (a) Measured and (b) calculated transmission spectrum of the $\text{Ta}_2\text{O}_5/\text{SiO}_2$ photonic crystal having nine-period lamination. The measured spectrum includes the reflection loss at the air-substrate boundary ($\sim 4\%$).

3. Application

3.1. BIREFRINGENCE

The dispersion relation of the 2D photonic crystals for propagation in the normal direction is calculated with the FDTD (finite-difference time-domain) method, as shown in Fig. 6 (Sato *et al.* 1999). The configuration of the unit cell is modeled on the SEM photograph. For simplicity, refractive indices are assumed to be wavelength-independent (2.25 for a high refractive index material (Ta_2O_5) and 1.48 for SiO_2). As a result of designing the structure

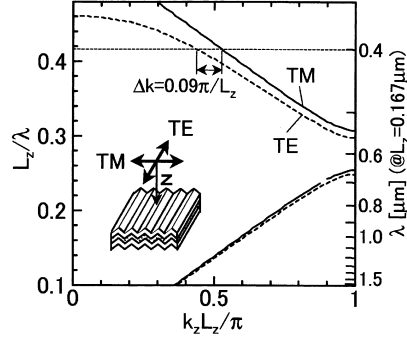


Fig. 6. Dispersion relation of the 2D photonic crystal for propagation normal to the substrate calculated with the FDTD method ($n_H = 2.25$, $n_L = 1.48$). The retardation at the wavelength of 400 and 430 nm are $0.091 \pi/L_z$ and $0.065 \pi/L_z$, respectively.

and the refractive index contrasts, there is a large difference in the wave-number (Δk_z) between the TE wave (polarized parallel to the grooves) and TM wave (polarized perpendicular to the grooves) in the second pass band ($L_z/\lambda = 0.30 - 0.42$). Therefore, it can be used as a birefringent element such as a waveplate.

The birefringence of the crystal is evaluated by the retardation when a light beam polarized at 45° to the grooves is transmitted normal to the substrate. Fig. 7(a) and (b) show the change of the state of polarization between the input and the output light. The retardation for a sample having 10-period lamination is 0.87π at the wavelength of 400 nm and the retardation for a sample having nine-period lamination at 430 nm is 0.53π , which agree well with the calculations. The results indicate the approximate operation as a half-wave plate and a quarter-wave plate, respectively. The retardation can be designed for an arbitrary wavelength by appropriately setting the number

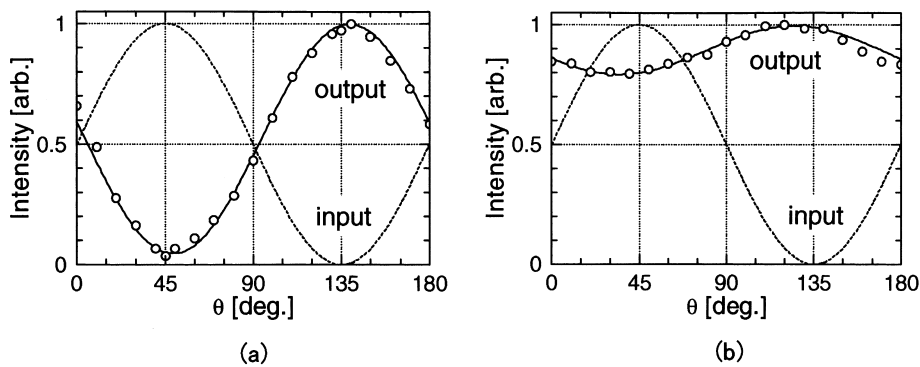


Fig. 7. State of polarization of the input and the output when light polarized at 45° to the grooves is injected normal to the $\text{Ta}_2\text{O}_5/\text{SiO}_2$ photonic crystal. (a) At $\lambda = 400$ nm, and (b) at $\lambda = 430$ nm.

of laminations and the layer thickness, therefore, practical half-wave and quarter-wave plates will be obtained.

The features of the artificial birefringent elements are as follows. The photonic crystals are composed of inexpensive, stable dielectric materials and their birefringence is as large as that of LiNbO_3 , which is 10 times larger than that of SiO_2 crystals. Moreover, arbitrary patterning of the birefringence is available by drawing initial grooves. As compared with conventional line-and-space (Aoyama *et al.* 1991; Xu *et al.* 1996), the fabrication process is stable and reproducible even if the pitch is less than $0.2 \mu\text{m}$ because irregularity in the initial pattern, if it exists, is automatically healed in the auto-cloning process (Kawashima 2000). This results in low-loss light propagation and high tolerance of fabricating the patterned substrates.

3.2. POLARIZATION SELECTIVE GRATING

As an example of an arbitrary drawing of birefringence, we demonstrate a polarization selective grating having flat regions and corrugated regions periodically, as shown in Fig. 8. According to the dispersion relation as shown in Fig. 9, the dispersion of the flat multilayer (1D periodic structure) is similar to that of the x -polarized wave (TM wave) for the 2D photonic crystal. Therefore, the proposed structure acts as a phase grating for only the y polarization. By adjusting the phase difference to π , the grating can separate the y polarization from the x polarization by first-order diffraction.

We fabricated the gratings composed of $\text{TiO}_2/\text{SiO}_2$ and $\text{Ta}_2\text{O}_5/\text{SiO}_2$ by stacking multilayers on a substrate with grooved regions and flat regions. The pitch of grooves is $0.24 \mu\text{m}$ and the constant of the phase grating is $6 \mu\text{m}$. The period of lamination and the number of lamination are $0.20 \mu\text{m}$ and 10 for $\text{TiO}_2/\text{SiO}_2$ and $0.23 \mu\text{m}$ and 13 for $\text{Ta}_2\text{O}_5/\text{SiO}_2$, respectively. Fig. 10(a) shows the cross-sectional SEM photograph of the grating, which indicates

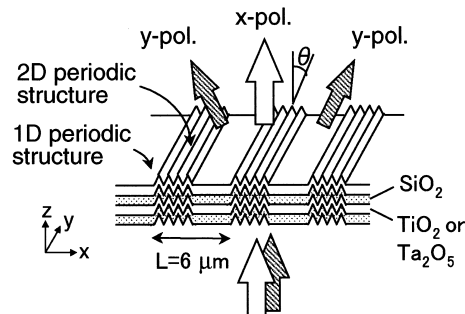


Fig. 8. Schematic illustration of polarization selective grating consisting of 2D photonic crystal and flat multilayer.

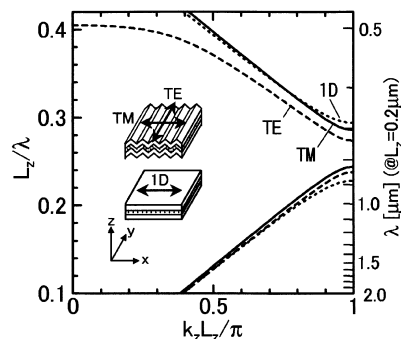


Fig. 9. Dispersion relation of 2D photonic crystal and a flat multilayer calculated with the FDTD method ($n_H = 2.3$, $n_L = 1.5$).

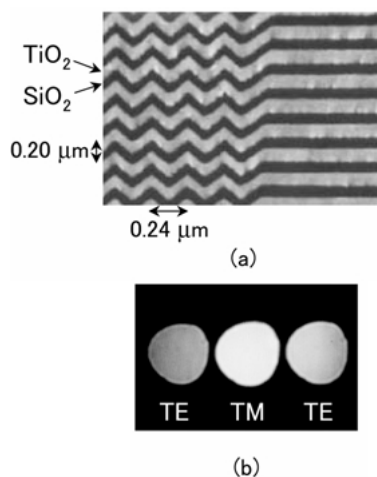


Fig. 10. (a) Cross-sectional SEM photograph of the polarization selective grating composed of $\text{TiO}_2/\text{SiO}_2$. (b) Diffraction pattern of the $\text{Ta}_2\text{O}_5/\text{SiO}_2$ grating when an incident light beam is polarized at 45° to the grooves ($\lambda = 523 \text{ nm}$). The measured splitting angle is 5° .

the boundary between a flat region and a corrugated region grows almost normal to the substrate.

The optical power transmitted through the grating is observed, as shown in Fig. 10(b), when an optical beam ($\lambda = 523 \text{ nm}$) polarized at 45° to the grooves is injected. We confirm the fundamental operation that the x -polarized wave is transmitted straight while the y -polarized wave is separated by the first-order diffraction. The splitting angle is measured to be 5° , which agrees well with the calculation. As compared with conventional phase gratings (Ohba *et al.* 1989; Aoyama *et al.* 1991; Xu *et al.* 1996), the elements have several advantages such as (a) use of inexpensive, stable materials, (b) reliable fabrication, and (c) a small thickness and a large splitting angle.

These advantages are emphasized when the wavelengths as short as 400 nm are used. Accordingly, the polarization splitters will be useful for optical pick-ups especially using a violet-range wavelength.

4. Summary

We have fabricated $\text{TiO}_2/\text{SiO}_2$ and $\text{Ta}_2\text{O}_5/\text{SiO}_2$ photonic crystals for the visible range by the autocloning technique and verified that the method offers flexible choice of materials and size. The photonic crystals can be applied to birefringent elements such as waveplates and polarization selective gratings by utilizing their large birefringence in the second pass band. These are useful for components such as optical pick-ups especially using a violet-range wavelength.

Acknowledgements

The authors would like to thank Prof O. Hanaizumi and Dr T. Kawashima for their helpful discussions. Part of this study was sponsored by the Special Correlation Funds for Promoting Science and Technology from the Science and Technology Agency, the Telecommunications Advancement Organization of Japan (TAO), and a grant-in-aid for Scientific Research (B) from the Japan Society for the Promotion of Science.

References

- Aoyama, S. and T. Yamashita. *Proc. SPIE* **1545** 241, 1991.
- Kawakami, S. *Electron. Lett.* **33** 1260, 1997.
- Kawakami, S., T. Kawashima and T. Sato. *Appl. Phys. Lett.* **74** 463, 1999.
- Kawashima, T., K. Miura, T. Sato and S. Kawakami. *Appl. Phys. Lett.* **77** 2613, 2000.
- Kosaka, H., T. Kawashima, A. Tomita, M. Notomi, T. Tamamura, T. Sato and S. Kawakami. *Phys. Rev. B* **58** R10096, 1998.
- Ohba, A., Y. Kimura, S. Sugama, Y. Urino and Y. Ono. *Jpn. J. Appl. Phys.* **28**(Suppl 28-3) 359, 1989.
- Ohtera, Y., T. Sato, T. Kawashima, T. Tamamura and S. Kawakami. *Electron. Lett.* **35** 1271, 1999.
- Sato, T., K. Miura, Y. Ohtera, T. Kawashima and S. Kawakami. *Trans. Instit Electr. Inform. Commun. Eng.* **J82-C-I** 572, 1999.
- Xu, F., R. Tyan, P. Sun, Y. Fainman, C. Cheng and A. Scherer. *Opt. Lett.* **21** 1513, 1996.
- Yablonovitch, E. *J. Opt. Soc. Am. B* **10** 283, 1993.